Application of fractional order PI controllers on a magnetic levitation system

Erhan YUMUK, Müjde GÜZELKAYA***, İbrahim EKSİN**
Department of Control and Automation Engineering, Faculty of Electrical and Electronics Engineering,
İstanbul Technical University, İstanbul, Turkey

Abstract: Fractional order PI controllers based on two different analytical design methods are applied to a magnetic levitation system in this paper. The controller parameters are specified in order to fulfill specific frequency criteria. The first design method utilizes a unity feedback reference model whose forward path includes Bode's ideal loop transfer function. The second method uses the reference model that has been obtained via delayed Bode's ideal loop transfer function. The achievement of these two controllers are contrasted with each other on the magnetic levitation system using various criteria.

Key words: Magnetic levitation system, delayed ideal Bode's loop, ideal Bode's loop, fractional order model, fractional order PI controllers

1. Introduction

Fractional calculus has been a continuing subject for more than three centuries and its utilization in the field of control system design is an up-to-date issue. The modeling and control of systems using fractional calculus provides certain advantages and flexibility when compared with their integer-order counterparts [1]. There exist three more cases with regard to the class of controllers and system models in the usage of fractional calculus, i.e. integer-order control for fractional-order models [2] and fractional-order control for integer-order models [3–7] and fractional-order models [8, 9].

The behavior of real-time systems are often expressed using higher-order differential equations. These higher order models may be approximated to the low integer order with time delay models [10]. However, these low-order models cannot represent the dynamics of the higher order systems accurately. Therefore, the controllers developed using these low-order models exhibit inadequate closed loop performances. Their fractional-order counterparts characterize the dynamic behavior of these systems more precisely because they have an additional parameter (i.e. fractional order) [1, 11–13]. Therefore, integer-order or fractional-order controllers developed based on these fractional-order models would be more realistic. Moreover, fractional-order controllers would also be a good choice due to their some additional parameters (e.g., fractional integrator or derivative orders). The fractional controller design methods are commonly based on frequency domain criteria such as phase margin (ϕ_m) and gain crossover frequency (ω_c). These methods are categorized into two parts: numerical [13, 14] and analytical methods [8, 9, 15].

There exist various application areas in which fractional calculus is utilized in control and modeling of systems. One of the most crucial application areas is magnetic levitation systems. Magnetic levitation systems

---

*Correspondence: guzelkaya@itu.edu.tr

are extensively employed in numerous areas such as magnetic levitation trains, rocket launch, artificial heart pumps, and magnetic levitation-based fans [16, 17]. Since magnetic levitation systems possess intrinsically nonlinear dynamics and unstable structure, the modeling and control of these systems are tough issues. Thus, both linear and nonlinear techniques have been developed for various dynamics models [18–21].

Two fractional-order PI controllers which use two different analytical design methods [8, 9] are applied to a magnetic levitation system in this study. In these analytical design methods, a type of fractional order model is used. The parameters of controllers are designated in order to fulfill specific frequency domain criteria. The first design method utilizes a unity feedback reference model whose forward path obtains Bode's ideal loop (BIL) transfer function [8]. In the second method, the reference model is obtained utilizing delayed BIL transfer function in the forward path [9]. The success of these two controllers are examined on a magnetic levitation system using various specifications. In this respect, we have shown that these two analytical controller design methods could be implemented successfully on a highly nonlinear system.

The rest of this paper is constructed as follows: Two fractional PI controller design methods are offered in Section 2. Section 3 gives the description and modeling of the magnetic levitation system. In Section 4, the controllers' design and their performance comparisons are included. Consequently, discussions and conclusions are given in Section 5.

2. Fractional PI controllers' design methods and their realizations

The unity feedback control system whose forward path includes $L(s)$ is considered as Figure 1a illustrates. The desired closed-loop transfer function might be described as follows:

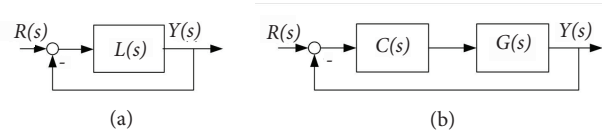$$P_{ref}(s) = \frac{L(s)}{1 + L(s)}. \tag{1}$$

Figure 1. (a) The reference system and (b) the control system block diagrams.

The transfer function of system ($P_{ref}(s)$) given in (1) is used as a reference model for any classical control system illustrated in Figure 1b with the transfer function $P(s)$ of the overall system as follows:

$$P(s) = \frac{C(s)G(s)}{1 + C(s)G(s)} \tag{2}$$

Here, $G(s)$ and $C(s)$ denote a system model and a controller, respectively. The controller $C(s)$ is determined in order that $P(s)$ imitates $P_{ref}(s)$ as much as possible.

The dynamics of higher-order processes may be characterized by fractional order structures. A higher-order transfer function might be represented by the fractional order model given as

$$G(s) = \frac{K_f}{\tau s^{\beta} + 1} e^{-\theta s}. \tag{3}$$

In this manner, a higher-order process is expressed by only four system model parameters $(K_f, \tau, \beta, \theta)$. On the other hand, the general transfer function of fractional order PI controller is described as

$$C(s) = H(s)K_p \left(1 + \frac{1}{T_i s^\lambda}\right) \tag{4}$$

where K_p, T_i, and λ denote the controller gain, time constant of integrator, and integrator order, respectively. $H(s)$ is the fractional filter.

2.1. The method based on Bode's ideal loop transfer function

Here, we first consider the method presented in [8], which will be referred to as Method I hereafter. This structure relies on internal model control (IMC). It is asserted in the literature that an IMC structure requires fewer parameters than other classical structures. In this respect, $L(s)$ given in Figure 1a is offered as BIL transfer function [22] as follows:

$$L(s) = \frac{K}{s^\gamma} \tag{5}$$

where $\gamma \in \mathbb{R}$ and K are the fractional order and the gain of system, respectively. BIL transfer function in Eq. (5) for $\gamma > 0$ and $\gamma < 0$, respectively, describes fractional-order integrator and differentiator.

The controller $C(s)$ in Figure 1b has to fulfill the following four specifications:

1. Gain crossover frequency (ω_c): $|C(j\omega_c)G(j\omega_c| = 1$.

2. Phase margin (ϕ_m): $Arg(C(j\omega_c)G(j\omega_c)) = -\pi + \phi_m$.

3. Elimination of the steady-state error (SSE): SSE is eliminated by using fractional-order integrator.

4. Flat phase: The open loop system phase is flat around ω_c. It is employed for robustness purposes.

$$\frac{dC(j\omega)G(j\omega)}{d\omega}\Big|_{\omega=\omega_c} = 0.$$

Note that SSE specification is met in case of $\gamma \geq 1$. When $\gamma < 1$, BIL transfer function is implemented as $\frac{Ks^{1-\gamma}}{s}$ to eliminate steady-state error.

When ω_c and ϕ_m are given, γ and K in Eq. (5) are determined via the formulas below:

$$\gamma = \frac{\pi - \phi_m}{\pi/2} \tag{6}$$

and

$$K = \omega_c^\gamma \tag{7}$$

The internal model control(IMC) structure illustrated in Figure 2 is utilized to design a controller. In this figure, $C_{IMC}(s)$ and $G(s)$ denote internal model controller and system model, respectively. The IMC controller is easily transformed into classical controller in Figure 1b using the following formula:

$$C(s) = \frac{C_{IMC}(s)}{1 - C_{IMC}(s)G(s)}. \tag{8}$$

The design of IMC controller consists of two stages:

- Stage 1: The model is separated into two parts:

$$G(s) = G_{mp}(s)G_{nmp}(s). \tag{9}$$

Here, $G_{mp}(s)$ and $G_{nmp}(s)$ denote minimum phase and nonminimum phase parts of model, respectively. Moreover, $G_{nmp}(s)$ has a steady-state gain of one.

- Stage 2: The controller is found using the following formula:

$$C_{IMC}(s) = \frac{M(s)}{G_{mp}(s)}. \tag{10}$$

Here, $M(s)$ is a reference model with unity gain.

In this case, when the following process model and reference model are utilized:

$$G(s) = \underbrace{\frac{K_f}{\tau s^\beta + 1}}_{G_{mp}(s)} \underbrace{e^{-\theta s}}_{G_{nmp}(s)}, \quad M(s) = \frac{K}{s^\gamma + K}, \tag{11}$$

the following IMC-type controller $(C_{IMC}(s))$ is obtained:

$$C_{IMC}(s) = \frac{K(\tau s^\beta + 1)}{K_f(s^\gamma + K)}. \tag{12}$$

The controller can be rewritten for the classical control system with unity feedback using Eq. 8 and the Taylor approximation of the time delay of model:

$$C_1(s) = \frac{K(\tau s^\beta + 1)}{K_f(s^\gamma + K\theta s)} \tag{13}$$

This controller may be organized in the following form:

$$C_1(s) = \underbrace{\frac{s^{\beta-1}}{1 + (1/K\theta)s^{\gamma-1}}}_{fractional\,filter} \underbrace{\frac{\tau}{K_f\theta}\left(1 + \frac{1}{\tau s^\beta}\right)}_{PI^\beta} \tag{14}$$
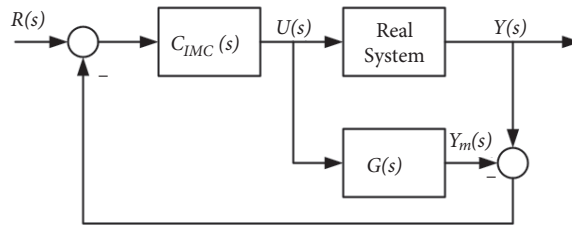

Figure 2. Block diagram of internal model control.

2.2. The method based on Bode's ideal loop transfer function plus time delay

Secondly, we consider another method presented in [9], which will be referred to as Method II thereon after. In this method, $L(s)$ given in Figure 1a is offered as delayed BIL transfer function as the following:

$$L(s) = \frac{K}{s^\gamma} e^{-\theta s}.$$ (15)

Here, θ denotes the model's time delay in (3).

The following three criteria met by the controller $C(s)$ in Figure 1b are selected:

1. Gain crossover frequency (ω_c): $|C(j\omega_c)G(j\omega_c| = 1$.

2. Phase margin (ϕ_m): $Arg(C(j\omega_c)G(j\omega_c)) = -\pi + \phi_m$.

3. Elimination of the steady-state error: SSE is eliminated using fractional order integrator again.

When ω_c and ϕ_m are selected, and also θ is taken from fractional model, γ and K in (15) are respectively calculated via the following formulas:

$$\gamma = \frac{\pi - \phi_m - \omega_c\theta}{\pi/2}$$ (16)

and

$$K = \omega_c^\gamma.$$ (17)

SSE specification is again satisfied in case of $\gamma \geq 1$. When the integrator order is less than 1, it is eliminated as in the previous method.

By utilizing the inverse of the fractional model in (3) without time delay in addition to BIL transfer function, the controller is designed as follows:

$$C_2(s) = \frac{K(\tau s^\beta + 1)}{K_f s^\gamma}$$ (18)

$C_2(s)$ may be rewritten in the following form:

$$C_2(s) = \underbrace{s^{\beta-\gamma}}_{fractional\,filter} \underbrace{\frac{K\tau}{K_f}\left(1 + \frac{1}{\tau s^\beta}\right)}_{PI^\beta}$$ (19)

2.3. Realization of fractional order operator

Oustaloup filter approximation is used to implement fractional operator in this study, which is given by:

$$s^\alpha \approx \mathscr{O}(s^\alpha) = K' \prod_{k=1}^{N} \frac{s + \omega_k'}{s + \omega_k}.$$ (20)

Here N and $\alpha \in (0,1)$ denote the order of the filter and the fractional order, respectively. Moreover, the gain(K'), zeros(ω_k') and the poles(ω_k) of the filter are found by the following formulas:

$$K' = \omega_h^\alpha.$$

$$\omega_k' = \omega_l \left(\frac{\omega_h}{\omega_l} \right)^{\frac{2k-1-\alpha}{2N}},$$

$$\omega_k = \omega_l \left(\frac{\omega_h}{\omega_l} \right)^{\frac{2k-1+\alpha}{2N}}.$$

(21)

Here ω_l and ω_h denote the lower and upper frequency bound values, respectively. Throughout the study, the order and frequency interval in the Oustaloup approximation are chosen as 11 and $[10^3, \ 10^{-3}]$. These order and frequency interval values are considered to be adequate for a sufficient approximation of fractional order operator [25].

3. Magnetic levitation system

3.1. Description of magnetic levitation plant

Figure 3 illustrates the magnetic levitation plant (MAGLEV). The aim of this plant is to control a one-inch solid ball levitating in its magnetic field in the desired location. The MAGLEV is composed of three distinct parts. The upper part consists of a solenoid coil with a steel core, i.e. an electromagnet. The middle part contains a cell in which the magnetic ball is suspended in the gap. One of the poles of the electromagnet faces the top of a black post with a steel ball on it. The position of the ball is measured by a photo-sensitive sensor. The distance between the electromagnet pole face and the ball's top hemisphere is 14 mm. Finally, in the bottom part of the plant, the required system's conditioning circuitry is located. For example, gain and offset potentiometers, which belong to the ball position sensor, are situated to calibrate properly. It also includes a current resistor to measure the coil current.

3.2. Magnetic levitation system stabilization

MAGLEV is a single input-single output unstable plant. However, the methods given in the previous section are all applicable to stable systems. For this reason, unstable MAGLEV plant has to be stabilized in order to apply these methods. In this respect, a state feedback controller with integrator and a feed-forward structure is utilized. The control system block diagram is illustrated in Figure 4.

3.3. Fractional order modeling of stabilized magnetic levitation system

The step input ranging from 6.7 to 8.7 mm are applied to the system for system identification in time domain. The maximum overshoot (δ) and the rise time (T_p) of the system response are found as 0.18% and 0.121 s, respectively. The model parameters (K_f, τ, and β) in (3) are calculated by means of the rule extracted for time domain characteristics in [23]. There, maximum overshoot (δ) and rise time (T_p) are given as a function of fractional order β and crossover frequency ω_c. When $\omega_c = \tau^{\frac{1}{\beta}}$, these formulas are obtained as

$$\delta = 0.8(\beta - 1)(\beta - 0.75)$$

(22)

$$T_p = \frac{1.106(\beta - 0.255)^2 \tau^{\frac{1}{\beta}}}{\beta - 0.921}$$
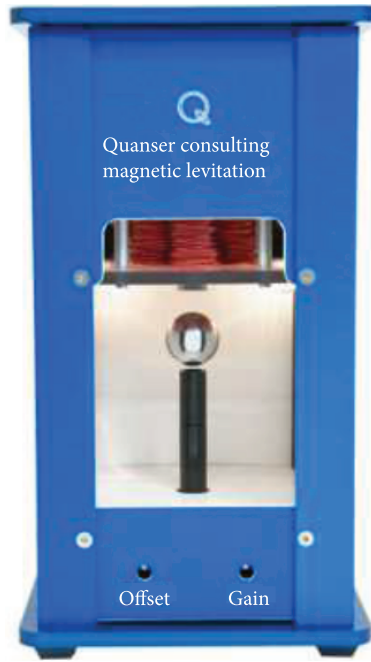
(23)

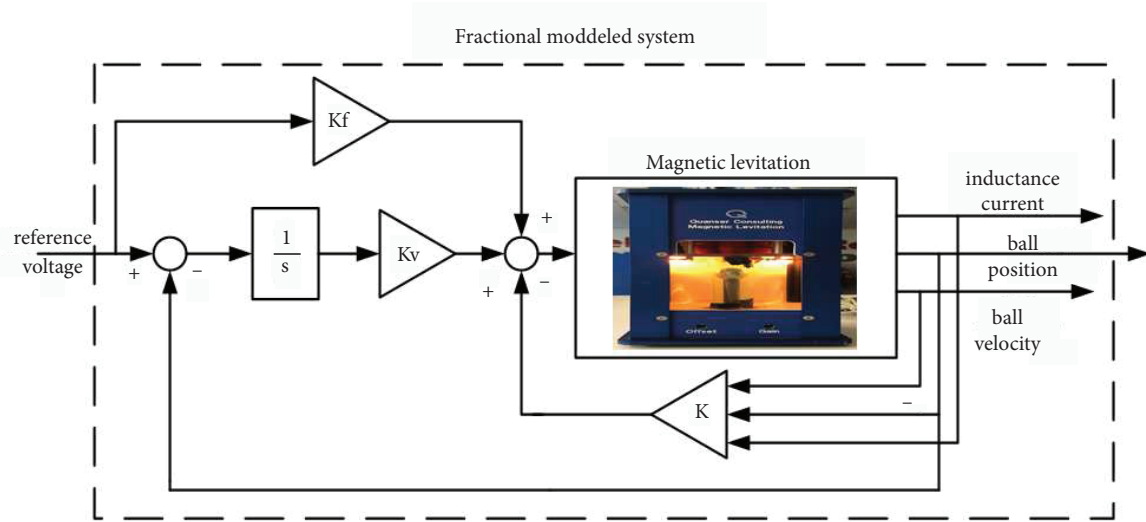**Figure 3**. Magnetic levitation system [24].

Figure 4. Magnetic levitation control system block diagram.

In that respect, the identified fractional model is as follows:

$$G(s) = \frac{1}{0.012s^{1.37} + 1} e^{-0.2s}. \tag{24}$$

Normalized root mean square error (NRMSE) between the output of the stabilized system in Figure 4 and the identified fractional model in (24) is calculated as 0.9323, which means very good fit since it is close to 1.

4. Design of fractional PI controllers

4.1. Controller parameters

Controllers are designed according to the following three different specifications set:

- Case I: $\omega_c = 2$ rad/s, $\phi_m = 30°$

- Case II: $\omega_c = 4$ rad/s, $\phi_m = 30°$

- Case III: $\omega_c = 2$ rad/s, $\phi_m = 60°$

Case I and Case II show how gain crossover frequency affects the closed-loop system performance while Case I and Case III demonstrate the effect of phase margin on the control system performance. Method I uses Eqs. (6) and (7) to calculate reference model coefficients in (5) while Method II utilizes Eqs. (16) and (17) to calculate reference model coefficients in (15), respectively. The calculated reference model parameters and designed controllers for each case are given in Table 1.

Table 1. Reference model and controller parameters.

	Method types	Parameters	Controllers
Case I	Method I	$\gamma = 1.667$ and $K = 3.174$	$\frac{0.06s^{0.37}}{1+1.575s^{0.667}}\left(1 + \frac{83.33}{s^{1.37}}\right)$
	Method II	$\gamma = 1.412$ and $K = 2.661$	$0.03193s^{-0.042}\left(1 + \frac{83.33}{s^{1.37}}\right)$
Case II	Method I	$\gamma = 1.667$ and $K = 10.080$	$\frac{0.06s^{0.37}}{1+0.496s^{0.667}}\left(1 + \frac{83.33}{s^{1.37}}\right)$
	Method II	$\gamma = 1.1574$ and $K = 4.975$	$0.0597s^{0.2126}\left(1 + \frac{83.33}{s^{1.37}}\right))$
Case III	Method I	$\gamma = 1.333$ and $K = 2.520$	$\frac{0.06s^{0.37}}{1+1.9843s^{0.333}}\left(1 + \frac{83.33}{s^{1.37}}\right)$
	Method II	$\gamma = 1.0787$ and $K = 2.112$	$0.02534s^{0.2913}\left(1 + \frac{83.33}{s^{1.37}}\right)$

4.2. Frequency responses of the controlled systems

The sinusoidal input signals are applied to the control system to acquire open-loop frequency response. The corresponding output signals of the closed-loop system are analyzed using fast Fourier transform. Then, the following formula are utilized to obtain the open-loop frequency response:

$$G(j\omega)C(j\omega) = \frac{T(j\omega)}{1 - T(j\omega)} \tag{25}$$

where $T(j\omega)$ and $C(j\omega)G(j\omega)$ are the frequency responses of the closed and open loop systems.

These frequency responses of control systems for Case I, II, and III are given in Figures 5a–5c, respectively. The corresponding frequency domain characteristics for these cases are given in Table 2. It could easily be observed that the frequency specifications are met better by Method II for all cases.

4.3. Time domain responses of the controlled systems

Figures 6a, 7a and 8a depict respectively the step time domain responses of the controlled systems for Case I, II, and III. Furthermore, the corresponding control signals are illustrated in Figures 6b, 7b, and 8b. Furthermore, Table 2 gives the corresponding time domain characteristics for all cases. It can be simply observed from these figures and the table that the control systems designed using Method II have less settling time, less rise time,
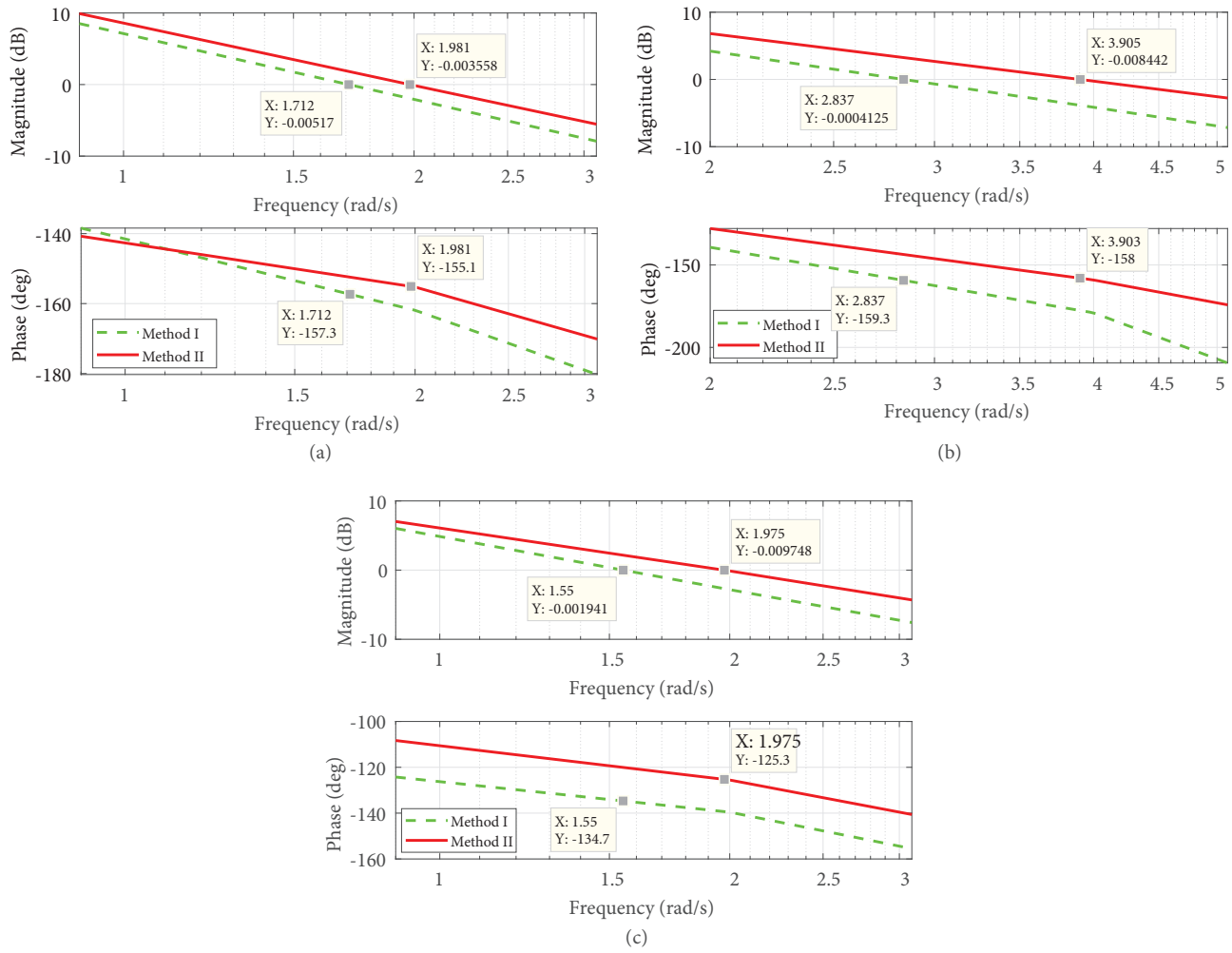
Figure 5. The controlled systems' frequency responses at (a) $\omega_c = 2$ rad/s, $\phi_m = 30°$, (b) $\omega_c = 4$ rad/s, $\phi_m = 30°$, (c) $\omega_c = 2$ rad/s, $\phi_m = 60°$.

Table 2. Frequency and time domain characteristics of control systems.

		ω_c (rad/s)	ϕ_m	M_p	t_s(s)	t_r (s)
Case I	Method I	1.712	22.7°	63.3	7.344	0.630
$\omega_c = 2$ rad, $\phi = 30°$	Method II	1.981	24.9°	63.6	5.098	0.461
Case II	Method I	2.837	20.7°	64.05	5.428	0.301
$\omega_c = 4$ rad, $\phi = 30°$	Method II	3.905	22.0°	68.21	4.538	0.235
Case III	Method I	1.550	45.3°	26.7	3.056	0.698
$\omega_c = 2$ rad, $\phi = 60°$	Method II	1.975	54.7°	15.0	2.160	0.491

and less or equal overshoot than the corresponding control system designed using Method I in terms of time domain characteristics. In addition, it can be said that the overshoot is dependent more on phase margin, rise time depends more on cut-off frequency, and settling time relies on both specifications.
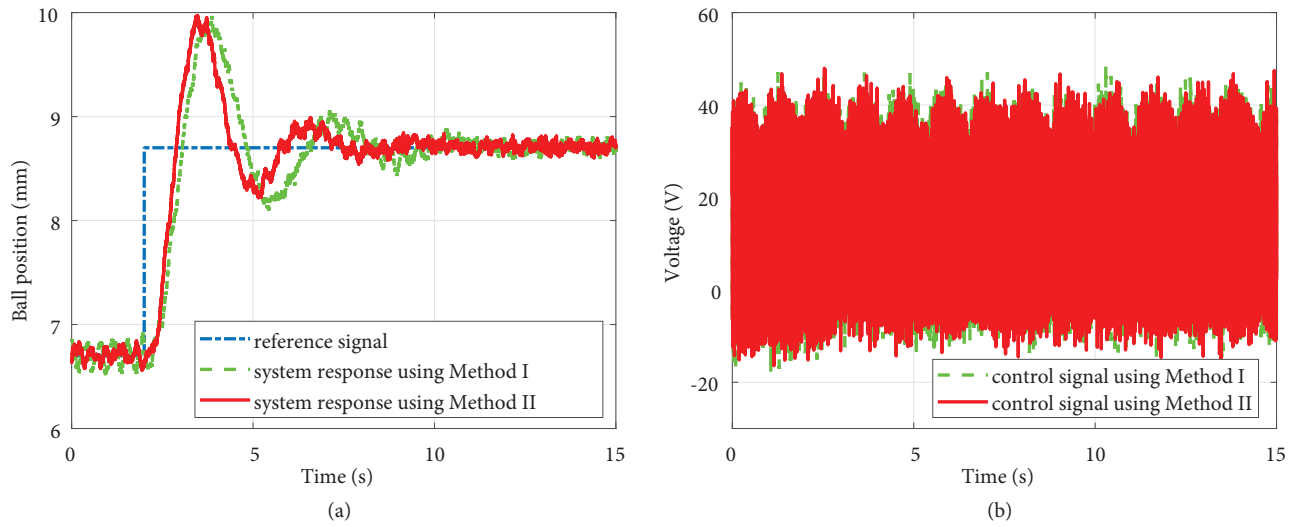
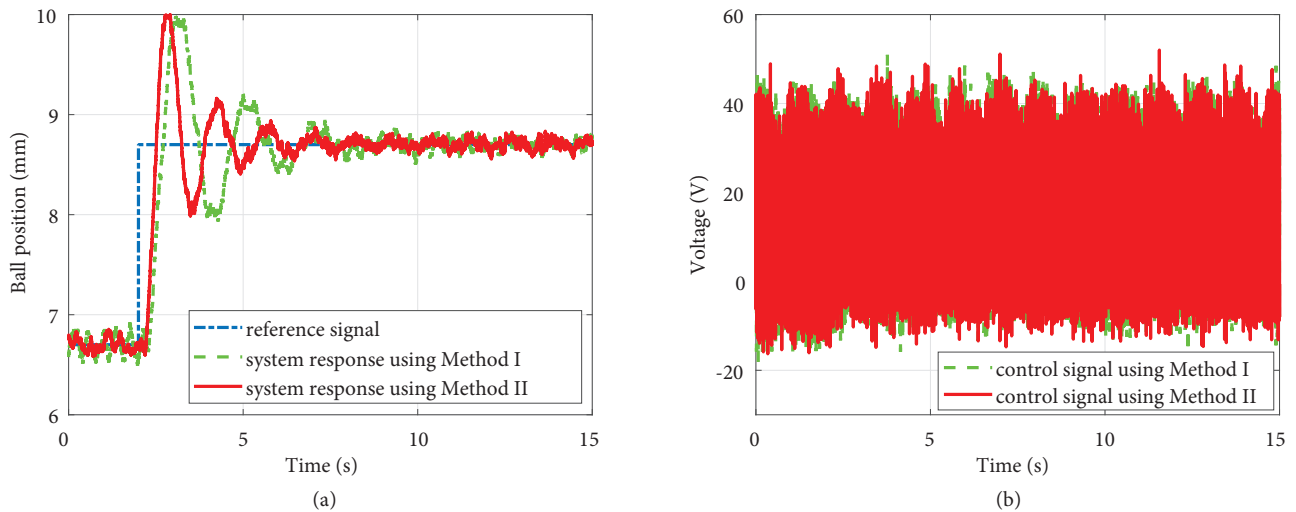**Figure 6**. (a)The output responses and (b) control signals for ($\omega_c = 2$ rad/s, $\phi_m = 30°$).

Figure 7. (a) The output responses and (b) control signals for ($\omega_c = 4$ rad/s, $\phi_m = 30°$)

5. Conclusion

In this study, we have shown the practicality of two different fractional order PI controllers based on basically BIL transfer function. These controllers are applied to a magnetic levitation system, which is intrinsically unstable. To apply these controllers, firstly, a state feedback is applied for stabilization. The consequent stabilized system with measurement delays is more adequate for modeling in a special fractional order form. Three frequency domain specifications are chosen to specify the controller design parameters. The outcoming controllers are applied to the real-time system and their performance in meeting the specifications are compared with each other. It is observed that the design specifications are satisfied much better by Method II. In terms of their time domain characteristics, the control systems designed using Method II have less settling time, less rise time, and less or equal overshoot than the corresponding control system designed using Method I.
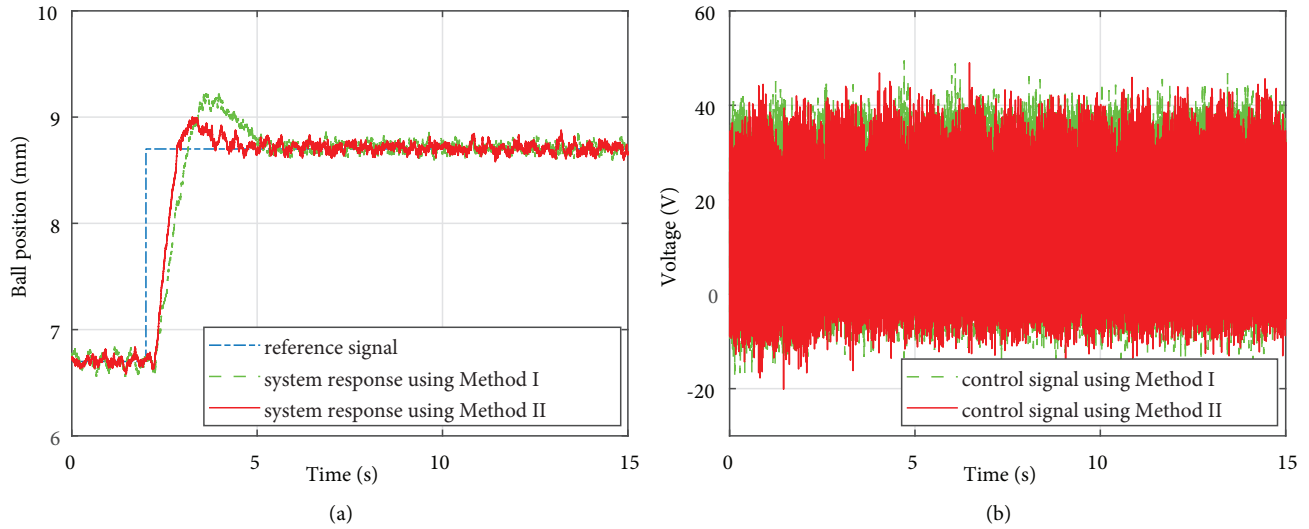
Figure 8. (a) The output responses and (b) control signals for $(\omega_c = 2 \text{ rad/s}, \phi_m = 60°)$

Acknowledgment

References

[1] Azarmi R, Tavakoli-Kakhki M, Sedigh, AK, Fatehi, A. Analytical design of fractional order PID controllers based on the fractional set-point weighted structure: Case study in twin rotor helicopter. Mechatronics 2015; 31: 376-388.

[2] Yumuk E, Guzelkaya M, Eksin I. Design of an integer order proportional–integral/proportional–integral–derivative controller based on model parameters of a certain class of fractional order systems. Proceedings of the Institution of Mechanical Engineers, Part I: Journal of Systems and Control Engineering 2019; 233; 3: 320-334.

[3] Saleem A, Soliman H, Al-Ratrout S, Mesbah M. Design of a fractional order PID controller with application to an induction motor drive. Turkish Journal of Electrical Engineering & Computer Sciences 2018; 26; 5: 2768-2778.

[4] Visioli A, Padula F. Tuning rules for optimal PID and fractional order PID controllers. Journal of Process Control 2011; 21: 69-81.

[5] Kurucu MC, Yumuk E, Güzelkaya M, Eksin İ. Investigation of the effects of fractional and integer order fuzzy logic PID controllers on system performances. In: IEEE 10th International Conference on Electrical and Electronics Engineering (ELECO); 2017; Bursa, Turkey. pp. 775-779.

[6] Kumar MR, Deepak V, Ghosh S. Fractional-order controller design in frequency domain using an improved nonlinear adaptive seeker optimization algorithm. Turkish Journal of Electrical Engineering & Computer Sciences 2017; 25; 5: 4299-4310.

[7] Titouche K, Mansouri R, Bettayeb M, Al-Saggaf UM. Internal model control–proportional integral derivative– Fractional-order filter controllers design for unstable delay systems. Journal of Dynamic Systems, Measurement, and Control 2016; 138; 2: 021006.

[8] Bettayeb M, Mansouri R. Fractional IMC-PID-filter controllers design for non-integer order systems. Journal of Process Control 2014; 24: 261-271.

[9] Yumuk E, Güzelkaya M, Eksin İ. Analytical fractional PID controller design based on Bode's ideal transfer function plus time delay. ISA Transactions 2019; 91: 196-206.

[10] Skogestad S. Simple analytic rules for model reduction and PID controller tuning. Journal of Process Control 2003; 13; 4: 291-309.

[11] Malek H, Luo Y, Chen YQ. Identification and tuning fractional order proportional integral controllers for time delayed system with a fractional pole. Mechatronics 2013; 23: 746-754.

[12] Yumuk E, Güzelkaya M, Eksin İ. Fractional and integer models of a ball balancing table system based on its frequency domain response. In: 8th International Conference on Advanced Technologies (ICAT'19); Sarajevo, Bosnia Herzegovina; 2019. pp. 1-6.

[13] Das S, Saha S, Das S, Gupta A. On the selection of tuning methodology of FOPID controllers for the control of higher order processes. ISA Transactions 2011; 50; 3: 376-388.

[14] Monje CA, Vinagre BM, Feliu V, Chen YQ. Tuning and auto-tuning of fractional order controllers for industry applications. Control Engineering Practice 2008; 16: 798-812.

[15] Luo Y, Chen Y. Fractional order [proportional derivative] controller for a class of fractional order systems. Automatica 2009; 45; 10: 2446-2450.

[16] Muresan CI, Ionescu C, Folea S, De Keyser, R. Fractional order control of unstable processes: the magnetic levitation study case. Nonlinear Dynamics 2015; 80; 4: 1761-1772.

[17] Kim KB, Im SH, Um DY, Park GS. Comparison of magnetic levitation systems using ring-shaped permanent magnets. IEEE Transactions on Magnetics, 2019; 55; 7: 1-4.

[18] de Jesús Rubio J, Zhang L, Lughofer E, Cruz P, Alsaedi A, Hayat T. Modeling and control with neural networks for a magnetic levitation system. Neurocomputing 2017; 227: 113-121.

[19] Maji D, Biswas M, Bhattacharya A, Sarkar G, Mondal TK et al. Maglev system modeling and LQR controller design in real time simulation. In: 2016 International Conference on Wireless Communications, Signal Processing and Networking (WiSPNET); New York, USA; 2016. pp. 1562-1567.

[20] Stettinger G, Benedikt M, Horn M, Zehetner J, Giebenhain C. Control of a magnetic levitation system with communication imperfections: A model-based coupling approach. Control Engineering Practice 2017; 58: 161-170.

[21] He G, Li J, Cui P. Nonlinear control scheme for the levitation module of maglev train. Journal of Dynamic Systems, Measurement, and Control 2016; 138; 7: 074503.

[22] Bode HW. Network analysis and feedback amplifier design. United States of America: van Nostrand, 1945.

[23] Barbosa RS, Machado JT, Ferreira IM. Tuning of PID controllers based on Bode's ideal transfer function. Nonlinear Dynamics 2004; 38; 1-4: 305-321.

[24] Quanser Inc. Magnetic levitation experiment (User manual). 2008.

[25] Tepljakov A, Petlenkov E, Belikov J. FOMCOM: a MATLAB toolbox for fractional-order system identification and control. International Journal of Microelectronics and Computer Science 2011; 2; 2: 51-62.